Int. J. Electrochem. Sci., 9 **(2014)** 5416 - 5424

International Journal of
ELECTROCHEMICAL
SCIENCE
www.electrochemsci.org

PdSn/C Electrocatalysts with Different Atomic Ratios for Ethanol Electro-Oxidation in Alkaline Media

Sirlane G. da Silva, Mônica H. M. T. Assumpção, Júlio César M. Silva, Rodrigo F. B. De Souza, Estevam V. Spinacé, Almir O. Neto and Guilherme S. Buzzo [*]

Instituto de Pesquisas Energéticas e Nucleares, IPEN/CNEN-SP, Av. Prof. Lineu Prestes, 2242 Cidade Universitária, CEP 05508-900, São Paulo, SP, Brazil
[*]E-mail: gsbuzzo@gmail.com

Received: 15 April 2014 / *Accepted:* 12 June 2014 / *Published:* 16 July 2014

PdSn/C with different Pd:Sn atomic ratios (90:10, 80:20. 70:30, 60:40 and 50:50) were prepared by borohydride reduction and tested for ethanol electro-oxidation in alkaline media. X-ray diffractograms patterns of the obtained materials showed the characteristic peaks of face-centered cubic structure of Pd, however, the PdSn alloy formation was not observed for all electrocatalysts. Also, the peaks of metallic Sn or SnO_2 phases were not clearly observed in the diffractograms suggesting the formation of amorphous phases. The electro-oxidation of ethanol was studied by cyclic voltammetry and chronoamperometry at room temperature and PdSn/C (50:50) showed the best performance in these conditions. PdSn/C (50:50) and (90:10) were tested in single fuel cell at 75^{o}C and the highest power density was obtained with PdSn/C (90:10).

Keywords: PdSn/C electrocatalysts, borohydride reduction, ethanol electro-oxidation reaction

1. INTRODUCTION

Considering the world economy, there is great interest in obtaining new energy sources that combine high efficiency with reduction of environmental impacts [1, 2]. This way, there is a great interest in the use of renewable fuels and more efficient power sources such as direct alcohol fuel cells (DAFC) [3-6].

Among the fuels, ethanol has been considered an interesting fuel for DAFCs because it could be produced in large scale through the fermentation of biomass and it is less toxic than methanol [7-9]. However, many obstacles have to be overcome due to the difficulty in oxidizing ethanol molecules to CO_2 since it requires steps of adsorption, dehydrogenation, C–C bond breaking, and oxidation of the resulting CO and other CHx adsorbed intermediates [8].

Platinum based catalyst is considered the most suitable anode material for the oxidation of alcohols but because of the elevated price and limited resources, Pt cannot be used for large-scale applications. Moreover, pure platinum is poisoned by strongly adsorbed species like CO, generated during the dissociation of organic compounds, reducing its activity [10-12].

Furthermore, notable enhancement of the electrocatalytic activity of platinum has been observed by introducing a second metal [11]. For these reasons, binary catalysts and non-platinum-based catalysts have been tested as electrode materials so that fuel cell could be made with reasonable price [13-19].

Considering the use of non-platinum electrocatalysts, Pt and Pd have very similar properties such as: same group of the periodic table, same fcc crystal structure and similar atomic size. Moreover, the cost of palladium is lower than Pt and Pd is fifty times more abundant on the earth than Pt. Then, Pd could be a good substitute for Pt [12].

Also considering the use of binary structures, some authors observed [10, 20, 21] that Sn is able to adsorb water molecules dissociatively to form OH_{ads} species, resulting in CO_2 and CH_3COOH formation at lower potentials than Pt by oxidation of adsorbed CO and CH_3CO species, according to the bi-functional mechanism. Thus, Sn is suggested to modify the electronic structure of Pt by forming an alloy with it, which improves ethanol electro-oxidation.

Taking into account the use of non-platinum and bimetallic electrocatalysts, this work describes the use of PdSn/C with Pd/Sn in different atomic ratios (90:10, 80:20, 70:30 60:40 and 50:50), prepared by the borohydride reduction method, toward ethanol oxidation reaction in alkaline media. For this study, cyclic voltammetry, chronoamperometry and also tests in direct ethanol alkaline fuel cell were employed.

2. MATERIALS AND METHODS

PdSn/C materials (20 % of metal loading) at different Pd:Sn atomic ratios: 90:10, 80:20, 70:30, 60:40 and 50:50 were prepared by the borohydride reduction method [22-24] using $Pd(NO_3)_2 \cdot 2H_2O$ (Aldrich) and $SnCl_2 \cdot 2H_2O$ as metal sources. By this process, firstly the support (Vulcan XC72 - Cabot Corporation) was dispersed in an isopropyl alcohol/water solution (50/50, v/v). After that, under stirring, the metal sources were added and put in an ultrasonic bath for 5 minutes. Then, a solution of sodium borohydride into 0.1 mol L^{-1} KOH was added in one portion under stirring and the resulting solution was maintained for more 15 minutes. After this procedure, the resultant mixture was filtered and the solids washed with water and dried at 70 ºC for 2 hours.

The atomic ratios of Pd and Sn in the synthesized materials were measured by energy dispersive spectroscopy (EDS) by using a JEOL – JSM6010 LA equipment. After that, the materials were characterized by XRD using a Rigaku diffractometer model Miniflex II using Cu Kα radiation source (0.15406 nm) being the diffractograms recorded in the range of $2\theta = 20$ to 90° with a step size of 0.05° and a scan time of 2 s per step. Transmission electron microscopy (TEM) images were also carried out using a JEOL transmission electron microscope model JEM-2100 operated at 200 kV in order to obtain the morphology and distribution of the nanoparticles on the support.

Electrochemical measurements were performed using cyclic voltammetry and chronoamperometry at room temperature with a potentiostat/galvanostat PGSTAT 30. For these experiments, a conventional 3 electrodes cell was employed using as reference an Ag/AgCl homemade electrode and a Pt plate as the counter electrode. The work electrodes (geometric area of 0.5 cm^2 with a depth of 0.3 mm) were prepared using the thin porous coating technique [25], and the ethanol oxidation reaction was studied by voltammetry at a scan rate of 10 mV s^{-1} in a 1 mol L^{-1} KOH and also with a 1 mol L^{-1} ethanol solution, both saturated with N_2. Chronoamperometry were also performed at -0.35V during 1800 s.

Experiments using real conditions, in other words, experiments in direct ethanol fuel cells were also performed using a single cell with an area of 5 cm^2. The temperature was set to 75 ˚C for the fuel cell and 85 ˚C for the oxygen humidifier. All electrodes contained 1 mg of Pt per cm^2 in the anode and Pt/C Basf was used in the cathode. The electrocatalyst was painted over carbon cloth in the form of a homogeneous dispersion prepared using Nafion® solution (5 wt.%, Aldrich). After the preparation, the electrodes were hot pressed on both sides of a Nafion® 117 membrane at 125 ºC for 3 min under a pressure of 100 kgf cm^{-2}. Prior to use, the membranes were exposed to 6 mol L^{-1} KOH solution for 24 h. The fuel, a 2 mol L^{-1} ethanol in 2 mol L^{-1} KOH was delivered at 2.0 mL min^{-1}, and the oxygen flow was set at 150 mL min^{-1}. Polarization curves were obtained by using a potentiostat/galvanostat PGSTAT 302N Autolab.

3. RESULTS AND DISCUSSION

Fig. 1 shows XRD for all electrocatalysts prepared with different PdSn atomic ratios. In all XRD patterns a broad peak at 2θ about 25º was observed and assigned to the (022) reflection of the hexagonal structure of Vulcan XC 72 carbon [26, 27]. Furthermore, all diffractograms showed peaks at 2θ = 40º, 46º, 68º and 82º which respectively correspond to (111), (200), (220) and (311) reflections of Pd face centered cubic (fcc) crystal according to JCPDF# 88-2335 as already observed by other authors [26-28]. Nevertheless, no diffraction characteristic peaks for Sn or SnO_2 were clearly observed, what could be explained by many reasons: i) the SnO_2 low cristallinity; ii) the SnO_2 small particle size and iii) the main diffraction peaks of SnO_2 being overlaid with that of Vulcan structure [28]. Moreover, no changes in the lattice parameter were observed.

The average crystallite size of palladium nanoparticles were estimated using the Debye-Scherrer equation [29] and the Pd (111) plane, yielding Pd mean crystallite size values in the range of 3 - 4 nm (Fig. 1).

The compositions of all PdSn/C materials were confirmed by using the EDS analysis. Table 1 shows the composition of each electrocatalyst in study and by these experiments it was possible to affirm that all materials are in agreement with the theoretic composition.

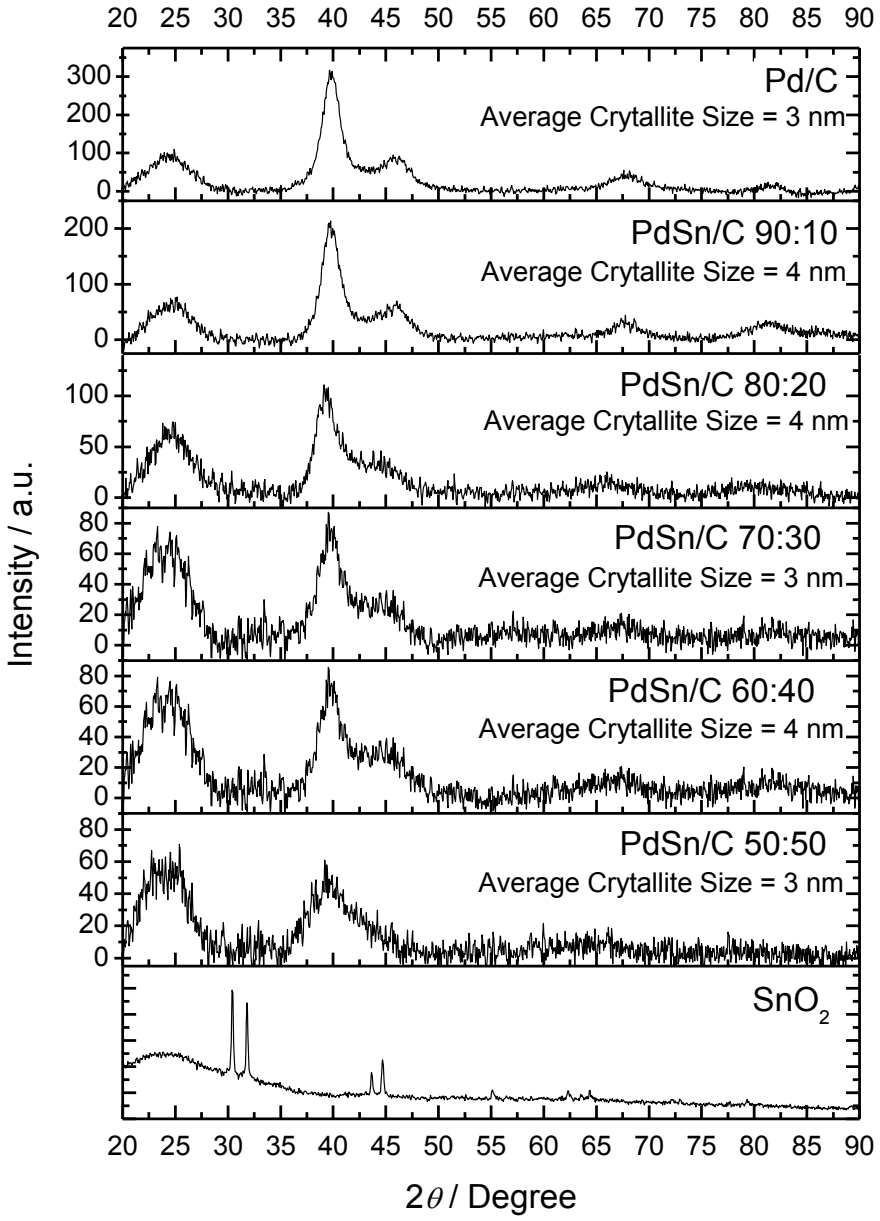

Figure 1. X-ray diffraction patterns of the PdSn/C electrocatalysts with crystallite average size.

Table 1. Atomic ratio of PdSn/C electrocatalysts.

Electrocatalyst	Atomic ratio from EDS (mol %)
PdSn/C (50:50)	PdSn 47:53
PdSn/C (60:40)	PdSn 64:36
PdSn/C (70:30)	PdSn 71:29
PdSn/C (80:20)	PdSn 79:21
PdSn/C (90:10)	PdSn 89:11

Cyclic voltammetry results for PdSn/C, Pd/C and Sn/C electrocatalysts in the absence of ethanol and in 1 mol L^{-1} KOH saturated with N_2 are shown in Fig. 2. From this figure it is possible to observe peaks associated with the hydrogen adsorption/desorption in the potential region of -0.85 to -0.45 V [30, 31]. Moreover, in the anodic oxidation, PdSn/C increases to yield a peak and then decreases while during the reverse scan a broad reduction peak is observed which represents the reduction of the Pd oxide layer [26, 28]. Accordingly to Modibedi *et al* [26] the voltammogram feature of Pd/C is similar to that of PdSn/C but both oxidation and reduction peaks are shifted positively by about 50 mV. This difference in the potential is due to the presence of Sn in Pd-Sn/C and was also observed on Fig. 2. PdSn electrocatalysts also yield different area (i.e. voltammetric charge) attributed to the formation of oxygen containing species, particularly OH species at Sn sites [30]

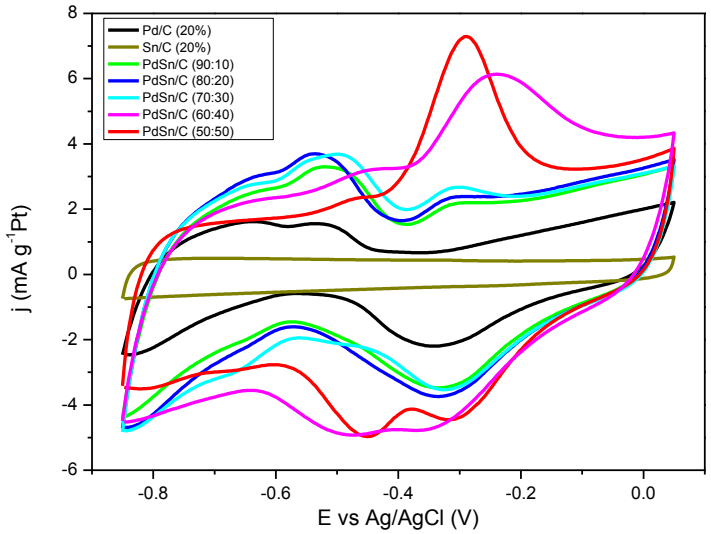

Figure 2. Cyclic voltammograms of the PdSn/C electrocatalysts in 1 mol L^{-1} KOH saturated with N_2 and scan rate of 10 mV s^{-1}.

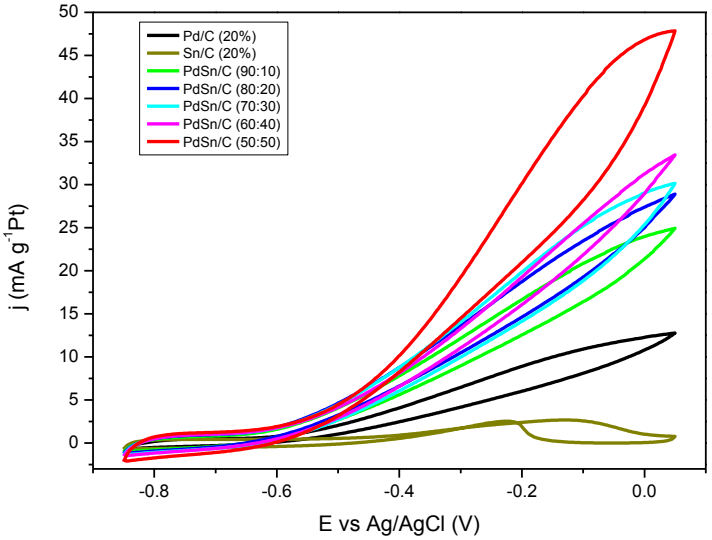

Figure 3. Cyclic voltammograms of PdSn/C electrocatalysts in presence of 1 mol L^{-1} ethanol and 1 mol L^{-1} KOH saturated with N_2 and scan rate of 10 mV s^{-1}.

Cyclic voltammograms of PdSn/C electrocatalysts in 1 mol L^{-1} ethanol solution at room temperature are presented on Fig. 3. The ethanol electro-oxidation on PdSn/C catalysts was characterized by one peak and the magnitude of this peak current indicates the electrocatalytic activity of the PdSn/C toward ethanol oxidation reaction. From these results, PdSn/C (50:50) showed the highest current density while Sn/C showed the lowest. Furthermore, PdSn/C (50:50) presented the lowest onset potential among the other catalysts in study.

Chronoamperometry show similar result in the electrocatalytic activity of the prepared nanocatalysts. Fig. 4 illustrates the stability of ethanol at -0,35 V on PdSn/C, Pd/C and Sn/C electrocatalysts. A gradual decrease in the oxidation current density with time was observed indicating the poisoning of the electrocatalysts; however, after the first 5 minutes a stable current density was observed for all catalysts and among them, PdSn/C (50:50) presented the highest current density, in accordance to voltammetry results.

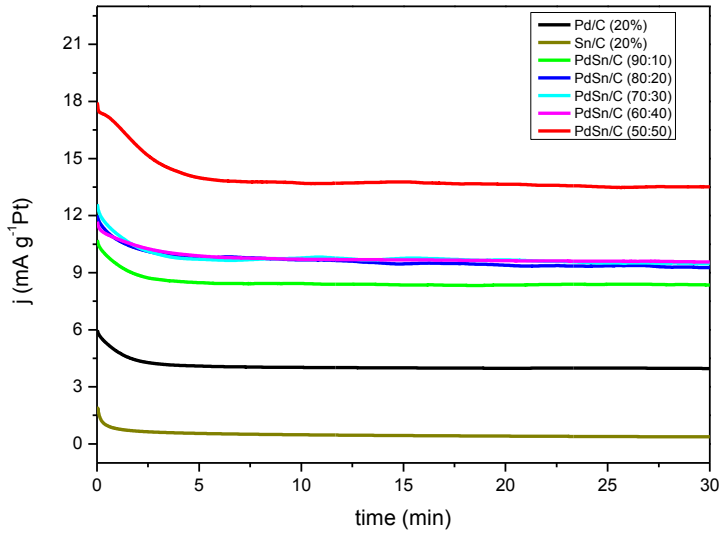

Figure 4. Current-time curves at – 0.35 V in presence of 1 mol L^{-1} ethanol and 1 mol L^{-1} KOH saturated with N_2 and room temperature.

Considering that by the XRD result no alloyed compound was formed, the best electrocatalytic activity observed with PdSn/C (50:50) could be attributed to the presence of oxophilic Sn species that improves the capability to remove adsorbed CO intermediate adsorbed (bi-functional mechanisms) since in the high pH value an oxide layer could be formed [32].

Additionally, it is known that the strongest effect of the bifunctional mechanism depends on achievement of the best ratio between the metals [33-35]. Also, Modibedi et al. [26] demonstrate that PdSn/C nanocatalyst is more active towards CO oxidation. Thus, it is reasonable that the highly enhanced activity of PdSn/C (50:50) could be attributed to a synergic effect of the compositions and the bi-functional mechanism caused by the presence of SnO_2 .

Furthermore, Liu *et al.* [36] studied the effect of the KOH concentration toward the ethanol oxidation and suggested that the kinetics of the ethanol oxidation reaction were improved by the greater availability of OH^- ions in solution and/or a higher OH^- coverage of the electrode surface.

Taking into account the use of the PdSn/C electrocatalysts in fuel cells, experiments in real conditions were also realized using PdSn/C (50:50) and PdSn/C (90:10) since the PdSn/C (50:50) showed the best electrocatalytic activity using electrochemical experiments but a lot of agglomerates by TEM images while PdSn/C (90:10) showed intermediate electrocatalytic activity but the best distribution of the nanoparticles on the carbon support (Fig. 5).

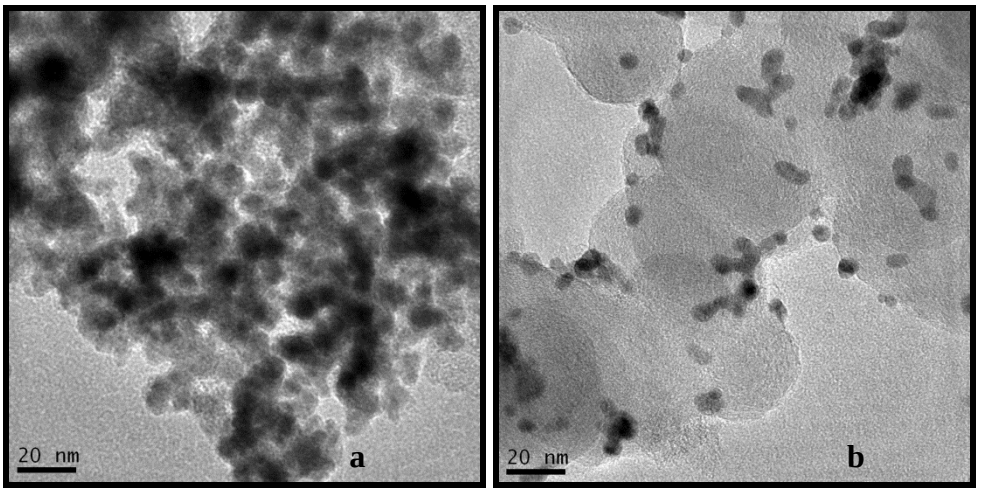

Figure 5. TEM images of a) PdSn/C (50:50) and b) PdSn (90:10) electrocatalysts.

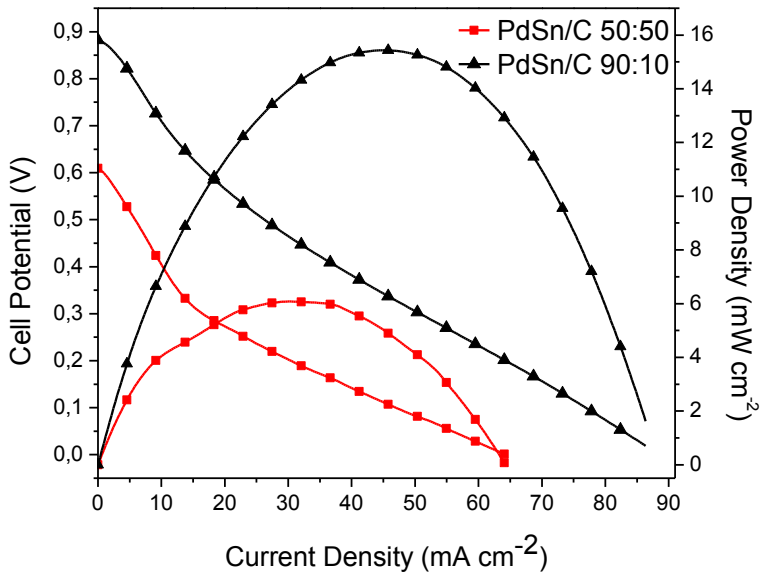

Figure 6. Polarization and power density curves of a 5 cm^2 direct ethanol fuel cell at 75 °C using 2 mol L^{-1} ethanol in 2 mol L^{-1} KOH and as anode a) PdSn/C (50:50) and b) PdSn/C (90:10). In both experiments the cathode used was Pt/C Basf (1mg Pt cm^{-2}).

The experiments of direct ethanol fuel cell are presented on Fig. 6. PdSn/C (50:50) showed the lowest open circuit voltage (OCV) and also the lowest current density (6 mW cm^{-2}) while PdSn/C (90:10) showed the highest OCV and also the highest current density (15 mW cm^{-2}), value more than twice higher when compared to PdSn/C (50:50).

Accordingly to Bonifácio *et al.* [37] more homogeneous electrocatalysts lead to higher membrane electrode assembly´s (MEA) performances. Moreover, it is known that the electrical resistance and the ability of the fuel in diffusing trough the MEA are factors that strongly influence the fuel cell efficiency [38-41] what could also contribute to the inversion of results obtained during fuel cell experiments since in the anode construction, there is a constant load of Pd (1 mg_{Pd} cm^{-1}) and consequently, the anode composed of PdSn/C (50:50) is thicker than the PdSn/C (90:10), yielding also more resistive electrode which hamper the fuel diffusion through the catalytic layer.

4. CONCLUSIONS

The borohydride reduction method was an efficient process to produce PdSn/C electrocatalysts for ethanol oxidation reaction. In all electrocatalysts peaks attributed to Pd fcc structure were observed, while peaks attributed to SnO_2 were not clearly observed. The electrocatalytic activity toward ethanol oxidation reaction in alkaline media showed that PdSn/C (50:50) electrocatalyst exhibited the highest current density, in accordance to the chronoamperometry. This result could be explained by the bi-function mechanism and by the improvement of the ethanol oxidation reaction in alkaline media. However, testes in fuel cell operation showed PdSn (90:10) as the most promising electrocatalysts since it presented the nanoparticles better dispersed on the support yielding the highest power density. However, effects of the electrical resistance and the fuel diffusion cannot be discarded. Further work is now necessary to investigate the electrocatalyst surface in order to elucidate the mechanism of ethanol electro-oxidation using these electrocatalysts.

ACKNOWLEDGMENTS
The authors wish to thank Laboratório de Microscopia do Centro de Ciências e Tecnologia de Materiais (CCTM) by TEM measurements, FAPESP (2011/18246-0, 2012/22731-4, 2012/03516-5, 2013/01577-0) and CNPq (150639/2013-9, 141469/2013-7) for the financial support.

References

1. E.M. Cunha, J. Ribeiro, K.B. Kokoh, A.R. de Andrade, *Int. J. Hydrogen Energ.*, 36 (2011) 11034.
2. A. Pérez, M. Montes, R. Molina, S. Moreno, *Appl. Catal. A-Gen*, 408 (2011) 96.
3. E. Antolini, *J. Power Sources*, 170 (2007) 1.
4. J.C.M. Silva, R.F.B. De Souza, L.S. Parreira, E.T. Neto, M.L. Calegaro, M.C. Santos, *Appl. Catal. B-Environ*, 99 (2010) 265.
5. M. Zhu, G. Sun, Q. Xin, *Electrochim. Acta*, 54 (2009) 1511.
6. E. Antolini, E.R. Gonzalez, *Appl. Catal. A- Gen*, 365 (2009) 1.
7. M.M. Tusi, N.S.O. Polanco, S.G. da Silva, E.V. Spinacé, A.O. Neto, *Electrochem. Commun*, 13 (2011) 143.
8. D.A. Cantane, W.F. Ambrosio, M. Chatenet, F.H.B. Lima, *J. Electroanal. Chem.*, 681 (2012) 56.

9. N.A.M. Barakat, M.A. Abdelkareem, H.Y. Kim, Applied Catalysis A: General, 455 (2013) 193-198.
10. J. Tayal, B. Rawat, S. Basu, *Int. J. Hydrogen Energ.*, 37 (2012) 4597.
11. S. Sen Gupta, S.S. Mahapatra, J. Datta, *J. Power Sources*, 131 (2004) 169.
12. E. Antolini, *Energ. Environ. Sci*, 2 (2009) 915.
13. H. Li, G. Sun, L. Cao, L. Jiang, Q. Xin, *Electrochim. Acta*, 52 (2007) 6622.
14. M. Li, A. Kowal, K. Sasaki, N. Marinkovic, D. Su, E. Korach, P. Liu, R.R. Adzic, *Electrochim. Acta*, 55 (2010) 4331.
15. H. Wang, X. Zhang, R. Wang, S. Ji, W. Wang, Q. Wang, Z. Lei, *J. Power Sources*, 196 (2011) 8000.
16. M. Li, W.P. Zhou, N.S. Marinkovic, K. Sasaki, R.R. Adzic, *Electrochim. Acta*, 104 (2013) 454.
17. L.S. Parreira, J.C.M. da Silva, M. D'Villa -Silva, F.C. Simões, S. Garcia, I. Gaubeur, M.A.L. Cordeiro, E.R. Leite, M.C. dos Santos, *Electrochim. Acta*, 96 (2013) 243.
18. J. Cai, Y. Huang, Y. Guo, *Electrochim. Acta*, 99 (2013) 22.
19. P.-C. Su, H.-S. Chen, T.-Y. Chen, C.-W. Liu, C.-H. Lee, J.-F. Lee, T.-S. Chan, K.-W. Wang, *Int. J. Hydrogen Energ.*, 38 (2013) 4474.
20. F. Colmati, E. Antolini, E.R. Gonzalez, *Appl.Catal.B-Environ.*, 73 (2007) 106-115.
21. W.J. Zhou, W.Z. Li, S.Q. Song, Z.H. Zhou, L.H. Jiang, G.Q. Sun, Q. Xin, K. Poulianitis, S. Kontou, P. Tsiakaras, *J. Power Sources*, 131 (2004) 217.
22. R.M. Piasentin, R.F.B. de Souza, J.C.M. Silva, E.V. Spinacé, M.C. Santos, A.O. Neto, *Int. J. Electrochem. Sci.*, 8 (2013) 435.
23. J.C. Castro, M.H.M.T. Assumpção, R.F.B. Souza, E.V. Spinacé, A.O. Neto, *Electrocatal.*, 4 (2013) 159.
24. J. Nandenha, R.F.B. Souza, M.H.M.T. Assumpção, E.V. Spinacé, A.O. Neto, *Ionics*, (2013) 1.
25. E.V. Spinacé, R. Dias, M. Brandalise, M. Linardi, A. Neto, *Ionics*, 16 (2010) 91.
26. R.M. Modibedi, T. Masombuka, M.K. Mathe, *Int. J. Hydrogen Energ.*, 36 (2011) 4664.
27. H. Wang, Z. Liu, S. Ji, K. Wang, T. Zhou, R. Wang, *Electrochim. Acta*, 108 (2013) 833.
28. Y. Ren, S. Zhang, H. Li, *Int. J. Hydrogen Energ.*, 39 (2014) 288.
29. A.W. Burton, K. Ong, T. Rea, I.Y. Chan, *Microporous Mesoporous Mater.*, 117 (2009) 75.
30. R. Awasthi, R.N. Singh, *Int. J. Hydrogen Energ.*, 37 (2012) 2103.
31. A.N. Geraldes, D.F. da Silva, E.S. Pino, J.C.M. da Silva, R.F.B. de Souza, P. Hammer, E.V. Spinacé, A.O. Neto, M. Linardi, M.C. dos Santos, *Electrochim. Acta*, 111 (2013) 455.
32. Q. He, W. Chen, S. Mukerjee, S. Chen, F. Laufek, *J Power Sources*, 187 (2009) 298.
33. J.C.M. Silva, B. Anea, R.F.B. De Souza, M.H.M.T. Assumpcao, M.L. Calegaro, A.O. Neto, M.C. Santos, *J. Brazil. Chem. Soc.*, 24 (2013) 1553.
34. G.A. Camara, R.B. de Lima, T. Iwasita, *Electrochem. Commun.*, 6 (2004) 812.
35. G.A. Camara, R.B. de Lima, T. Iwasita, *J. Electroanal. Chem.*, 585 (2005) 128.
36. J. Liu, J. Ye, C. Xu, S.P. Jiang, Y. Tong, *Electrochem. Commun.*, 9 (2007) 2334.
37. R.N. Bonifácio, J.O.A. Paschoal, M. Linardi, R. Cuenca, *J Power Sources*, 196 (2011) 4680.
38. A.R. Hind, S.K. Bhargava, A. McKinnon, *Adv. Colloid Interface Sci.*, 93 (2001) 91.
39. S. Song, Y. Wang, P. Shen, *Chinese J Catal.*, 28 (2007) 752.
40. R.F.B. De Souza, J.C.M. Silva, F.C. Simões, M.L. Calegaro, A.O. Neto, M.C. Santos, *Int. J. Electrochem. Sci.*, 7 (2012) 5356.
41. A.O. Neto, J. Nandenha, M.H.M.T. Assumpção, M. Linardi, E.V. Spinacé, R.F.B. de Souza, *Int. Journal Hydrogen Energ.*, 38 (2013) 10585.